blood

2011 117: 6024-6035
Prepublished online February 25, 2011;
doi:10.1182/blood-2010-10-311589

Ischemic neurons prevent vascular regeneration of neural tissue by secreting semaphorin 3A

Jean-Sébastien Joyal, Nicholas Sitaras, François Binet, Jose Carlos Rivera, Andreas Stahl, Karine Zaniolo, Zhuo Shao, Anna Polosa, Tang Zhu, David Hamel, Mikheil Djavari, Dario Kunik, Jean-Claude Honoré, Emilie Picard, Alexandra Zabeida, Daya R. Varma, Gilles Hickson, Joseph Mancini, Michael Klagsbrun, Santiago Costantino, Christian Beauséjour, Pierre Lachapelle, Lois E. H. Smith, Sylvain Chemtob and Przemyslaw Sapieha

Blood (print ISSN 0006-4971, online ISSN 1528-0020), is published weekly by the American Society of Hematology, 2021 L St, NW, Suite 900, Washington DC 20036.

Ischemic neurons prevent vascular regeneration of neural tissue by secreting semaphorin 3A

*Jean-Sébastien Joyal,[1,2] *Nicholas Sitaras,[2,3] François Binet,[3] Jose Carlos Rivera,[2] Andreas Stahl,[4] Karine Zaniolo,[2] Zhuo Shao,[1] Anna Polosa,[5] Tang Zhu,[2] David Hamel,[3] Mikheil Djavari,[5] Dario Kunik,[3] Jean-Claude Honoré,[2] Emilie Picard,[2] Alexandra Zabeida,[2] Daya R. Varma,[1] Gilles Hickson,[2] Joseph Mancini,[2,3] Michael Klagsbrun,[6] Santiago Costantino,[3] Christian Beauséjour,[2] Pierre Lachapelle,[5] Lois E. H. Smith,[7] Sylvain Chemtob,[1-3] and Przemyslaw Sapieha[3,8]

[1]Department of Pharmacology and Therapeutics, McGill University, Montreal, QC; [2]Departments of Pediatrics, Ophthalmology, and Pharmacology, CHU Sainte-Justine Research Center, University of Montreal, Montreal, QC; [3]Department of Ophthalmology, Maisonneuve-Rosemont Hospital Research Centre, University of Montreal, Montreal, QC; [4]Department of Ophthalmology, University of Freiburg, Freiburg, Germany; [5]Department of Ophthalmology and Neurology-Neurosurgery, McGill Montreal Children's Hospital Research Institute, McGill University, Montreal, QC; [6]Vascular Biology and [7]Department of Ophthalmology, Children's Hospital Boston, Harvard Medical School, Boston, MA; and [8]Department of Neurology-Neurosurgery, McGill University, Montreal, QC

The failure of blood vessels to revascularize ischemic neural tissue represents a significant challenge for vascular biology. Examples include proliferative retinopathies (PRs) such as retinopathy of prematurity and proliferative diabetic retinopathy, which are the leading causes of blindness in children and working-age adults. PRs are characterized by initial microvascular degeneration, followed by a compensatory albeit pathologic hypervascularization mounted by the hypoxic retina attempting to reinstate metabolic equilibrium. Paradoxically, this secondary revascularization fails to grow into the most ischemic regions of the retina. Instead, the new vessels are misdirected toward the vitreous, suggesting that vasorepulsive forces operate in the avascular hypoxic retina. In the present study, we demonstrate that the neuronal guidance cue semaphorin 3A (Sema3A) is secreted by hypoxic neurons in the avascular retina in response to the proinflammatory cytokine IL-1β. Sema3A contributes to vascular decay and later forms a chemical barrier that repels neo-vessels toward the vitreous. Conversely, silencing Sema3A expression enhances normal vascular regeneration within the ischemic retina, thereby diminishing aberrant neovascularization and preserving neuroretinal function. Overcoming the chemical barrier (Sema3A) released by ischemic neurons accelerates the vascular regeneration of neural tissues, which restores metabolic supply and improves retinal function. Our findings may be applicable to other neurovascular ischemic conditions such as stroke. (*Blood*. 2011;117(22):6024-6035)

Introduction

Proliferative retinopathies (PRs) are traditionally perceived as disorders limited to the microvasculature because of the characteristic profuse and deregulated growth of retinal vessels.[1] The mechanisms by which neovessels grow toward the vitreous and fail to revascularize ischemic zones are thought to result from high concentrations of proangiogenic factors such as VEGF in the vitreous of PR patients. However, if such an explanation were sufficient, retinal glial cells (astrocytes and Müller cells)[2] and neurons[3] that produce vast amounts of growth factors under hypoxic conditions should retain vessels on the retinal surface and ensure revascularization of the retina proper. It is, therefore, compelling to hypothesize the presence of a vasorepulsive force originating from the significantly hypoxic avascular retina that repels neovessels away from the vaso-obliterated retina and grows toward the vitreous.

Neurovascular cross-talk shapes vascular development but has received limited attention in the pathology setting. In PRs, evidence points to an early decline in the function of ischemic regions of the neural retina, as shown by multifocal electroretinogram (mfERG).[4,5] Throughout the vaso-obliterative phase of retinopathy, the local retinal environment is hostile to both vasculature and neurons.[6] After blood vessel degeneration, neurons are metabolically starved and undergo several adaptive cellular changes to counter the ischemic state of the tissue.[3,6] If adequate vascular supply is not reinstated in time to salvage deprived neurons, it is conceivable that these severely hypoxic cells may mount a repulsive front in an attempt to shunt metabolic resources away from the perishing ischemic tissue toward less affected regions of the retina. In the process, excessive production of VEGF[7] induces exaggerated neovascularization at the periphery of the ischemic and repulsive zones into the pre-retinal region (normally devoid of vasculature), because reestablishing a vascular network to neurons that are unsalvageable would be wasteful.

Given their established role in influencing endothelial cell (EC) behavior, classic neuronal guidance cues may mediate the misguided growth of neovessels away from the ischemic retina.[8] During embryonic development, nerves and blood vessels establish architecturally optimized networks to ensure adequate transmission of sensory information and tissue perfusion; of particular interest are the class III semaphorins such as Sema3A. Sema3A binds to

Submitted October 5, 2010; accepted February 9, 2011. Prepublished online as *Blood* First Edition paper, February 25, 2011; DOI 10.1182/blood-2010-10-311589.

*J.S.J. and N.S. contributed equally to this study.

An Inside *Blood* analysis of this article appears at the front of this issue.

The online version of this article contains a data supplement.

The publication costs of this article were defrayed in part by page charge payment. Therefore, and solely to indicate this fact, this article is hereby marked "advertisement" in accordance with 18 USC section 1734.

Neuropilin-1 (Nrp-1) to elicit (neuronal) cytoskeletal collapse.[9,10] In addition, $VEGF_{165}$ also binds to Nrp-1 to promote its angiogenic effects.[10-12] These opposing actions of Sema3A and VEGF, whereby Sema3A directly provokes EC apoptosis and inhibits VEGF-dependent chemotaxis, may be important contributors to the vascular phenotypes observed in PRs. Previous studies have demonstrated a role for Sema3A in vascular morphogenesis in developing embryos[13] and in the inhibition of angiogenesis during tumor growth.[14]

Using an oxygen-induced model of PR (oxygen-induced retinopathy [OIR]),[15,16] we demonstrate that the inflammatory environment present in the ischemic neural retina, notably involving IL-1β, induces robust production of Sema3A specifically in retinal ganglion neurons. Sema3A was found to contribute to vascular decay and curtail revascularization of the ischemic zones, resulting in misguided intravitreal vascular growth in ischemic retinopathies. Our findings reach beyond previously reported antiangiogenic properties of Sema3A, because we provide evidence for a counter-intuitive uncoupling of neuronal metabolism and vascular supply. We show that in response to hypoxia, neurons secrete a chemical barrier (Sema3A) to repulse new vessels and in turn prevent revascularization of hypoxic retinal tissue. Conversely, we demonstrate that rapid enhancement of retinal revascularization during the early ischemic stages effectively prevents aberrant pre-retinal neovascularization.

Methods

Animals

All studies adhered to the Association for Research in Vision and Ophthalmology (ARVO) Statement for the Use of Animals in Ophthalmic and Vision Research and were approved by the Animal Care Committee of the University of Montreal in accordance with the guidelines established by the Canadian Council on Animal Care. C57Bl/6 wild-type, GFP mice (C57BL/6-Tg UBC GFP 30Scha/J, stock number 004353) and RGC-YFP mice (B6.Cg-Tg Thy1-YFPH 2Jrs/J, stock number 003782) were purchased from The Jackson Laboratory.

OIR

This model serves as a proxy to human ocular neovascular diseases such as retinopathy of prematurity and diabetic retinopathy, which are characterized by a late phase of destructive pathologic angiogenesis.[1,17] Mice were exposed to 75% oxygen from postnatal day 7 (P7) to P12. On return to room air, hypoxia-driven neovascularization develops from P14 on.[15-18] Intravitreal injections were performed as follows. Twice-daily intraperitoneal injections of IL-1R antagonist (Kineret, 20 mg/kg; Biovitrum) were administered from P10 for 4 days. The eyes were collected at documented time points. Retinal vaso-obliteration was evaluated at P12, P14, and P17, whereas neovascularization was evaluated at the disease peak (P17), as described previously.[15] Briefly, mice were given a lethal dose of Avertin (Sigma-Aldrich) and eyes were enucleated and fixed in 4% paraformaldehyde for 1 hour at room temperature. Retinas were dissected and stained overnight at room temperature with fluoresceinated isolectin B4 (Alexa Fluor 594, I21413; Molecular Probes) in 1mM $CaCl_2$ in PBS. Lectin-stained retinas were whole-mounted onto Superfrost Plus microscope slides (Fisher Scientific) with the photoreceptor side down and imbedded in SlowFade Antifade Reagent (Invitrogen). For quantification of retinal neovascularization, 20 images of each whole-mounted retina were obtained at 5× magnification using fluorescence microscopy (Eclipse E800; Nikon). Vaso-obliterated areas were assessed as the retinal area devoid of vasculature over the total retinal retina. Neovascularization was analyzed using the SWIFT-NV method.[19] All mice weighing less than 5.5 g at P17 were excluded from the study to eliminate all runty animals.[20]

RT-PCR and real-time qRT-PCR analysis

Eyes were rapidly enucleated and whole retinas (or laser-captured retinal layers or vessels) processed for RNA using TRIzol (Invitrogen), followed by treatment with DNase I (QIAGEN) to remove any contaminating genomic DNA. The DNase-treated RNA was then converted into cDNA using M-MLV reverse transcriptase (Invitrogen). PCR primers targeting mouse and rat VEGFA, Sema3A, Sema3E, Sema3F, Nrp-1, IL-1β, IL-6, TNFα, and the control genes cyclophilin A and 18S were designed using Primer Bank and NCBI Primer Blast. Quantitative analysis of gene expression was generated using an ABI Prism 7700 sequence detection system and the SYBR Green Master Mix Kit (BioRad), and gene expression was calculated relative to cyclophilin A or 18S universal primer pair (Ambion) expression using the ΔCt method.

Western blot

Retinal samples were obtained as described in "OIR." Samples were centrifuged and 50 μg of pooled retinal lysate from a minimum of 3 different animals was loaded on an SDS-PAGE gel and electroblotted onto a PVDF membrane. After blocking, the membranes were incubated overnight with 1:200 rabbit antibody to mouse VEGFA (sc-152; Santa Cruz Biotechnology), 1:1000 rabbit antibody to mouse Sema3A (ab23393; Abcam); 1:1500 rabbit antibody to mouse IL-1RI (sc-689; Santa Cruz Biotechnology), 1:200 goat antibody to rat IL-1β (MAB501; R&D Systems); and 1:1000 mouse antibody to mouse β-actin (sc-47778; Santa Cruz Biotechnology). After washing, membranes were incubated with 1:5000 horseradish peroxidase–conjugated anti-rabbit, anti-goat, or anti-mouse secondary antibodies (Amersham) for 1 hour at room temperature. Bands were assessed using densitometry plug-ins in Image Pro 4.5 software (Media Cybernetics).

Laser capture microdissection

Eyes with OIR or normoxic controls were enucleated at P14 or P17 and embedded in optimal cutting temperature compound. The eyes were sectioned at 12 μm in a cryostat, mounted on RNase-free polyethylene naphthalate glass slides (11505189; Leica), and immediately stored at −80°C. Slides containing frozen sections were fixed in 50% ethanol for 15 seconds, followed by 30 seconds in 75% ethanol, before being washed with diethylpyrocarbonate-treated water for 15 seconds. Sections were stained with hematoxylin/eosin or fluoresceinated isolectin B4 (Alexa Fluor 594, I21413; Molecular Probes) at a 1:50 dilution in 1mM $CaCl_2$ in PBS, and treated with RNase inhibitor (03 335 399 001; Roche) at 25°C for 3 minutes. Layers or neovessels were laser-microdissected with the LMD 6000 system (Leica Microsystems) and collected directly into lysis buffer using the RNeasy Micro Kit (QIAGEN).

Immunohistochemistry

For immunohistochemistry, eyes were enucleated from mice and fixed in 4% paraformaldehyde at room temperature for 4 hours, incubated in 30% sucrose overnight, and then frozen in optimal cutting temperature compound. Sagittal cross-sections were permeabilized overnight at 4°C and incubated with rabbit IL-1RI (sc-689; Santa Cruz Biotechnology) or rabbit Sema3A (ab23393; Abcam) and mouse Thy1.1 (Millipore), followed by fluoresceinated secondary antibodies (goat anti–mouse IgG Alexa Fluor 594 and goat anti-rabbit IgG Alexa Fluor 488 and 594; Invitrogen) for localization studies according to the manufacturer's recommendations. Flat-mount retinas were stained with 0.1% Triton X-100 (T-8787; Sigma-Aldrich) in PBS and with fluoresceinated isolectin B4 (Alexa Fluor 594, I21413; Molecular Probes) in 1mM $CaCl_2$ in PBS for retinal vasculature. Antibodies to rabbit Nrp-1 (sc-5541; Santa Cruz Biotechnology) were applied overnight and secondary Abs were added. Samples were visualized using 40× objectives with fluorescence microscopy (Eclipse E800; Nikon).

Lentivirus production

Lentiviral vectors (HIV-1 derived) were prepared by transfecting HEK293T cells with a vector plasmid containing the small hairpin RNA (shRNA)

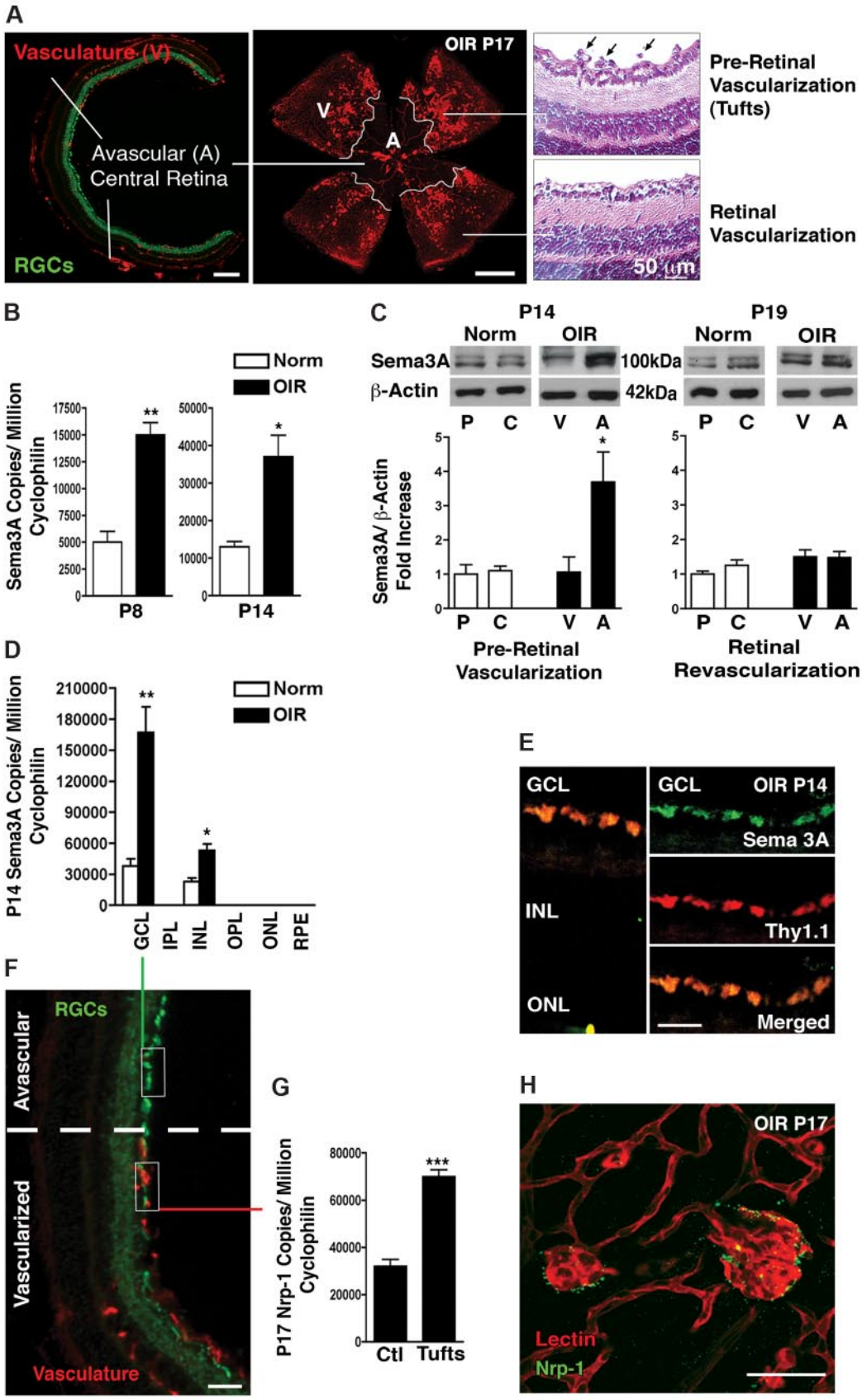

Figure 1. Sema3A expression is consistent with a role in retinopathy. (A) Frozen cross-section (left panel) and flat-mount retinas (central panel) taken at P17 of OIR demonstrating the principal characteristics of PRs including avascular (A) and vascular (V) zones. Paraffin sections (right panel) demonstrating pre-retinal neovascular tufts (black arrows). (B) Real-time PCR on whole retinas taken at P8 and P14 demonstrates an ~ 3-fold increase in Sema3A during the vaso-obliterative and neovascular phases of PRs, respectively (n = 3). Values are gene copy number normalized to *CyclophilinA* standards ± SEM. $^{**}P = .0015$ and $^{*}P = .0157$ compared with normoxia (Norm). (C) Microdissection of avascular regions of the OIR retina at P14 reveals a 3.5-fold induction in Sema3A protein levels in the avascular area (n = 3). Values are shown relative

against Sema3A or green fluorescent protein together with the third-generation packaging plasmids pV-SVG, pMDL, and pREV (Open Biosystems). Approximately 10^7 cells were seeded and transfected with the above plasmids in DMEM complete medium (Invitrogen) and incubated for 30 hours. Subsequently, supernatant was replaced with fresh complete DMEM medium and incubated for an additional 30 hours. Secreted virus was collected and ultracentrifuged at 50 000*g*, resuspended in PBS, aliquoted, and stored at −80°C.

Intravitreal injections

P2 or P14 C57BL/6 pups were anesthetized with 3.0% isoflurane and injected intravitreally with 0.5μL of lentivirus (see "Lentivirus production") or recombinant Sema3A (rSema3A, 100 ng/μL), respectively, using a 10-μL Hamilton syringe fitted with a 50-gauge glass capillary tip. Approximately 254 ± 11.0 ng/μL of lentivirus shGFP and 323.3 ± 15.3 ng/μL containing shSema3A was injected; virus titers were assessed with the p24 ELISA kit (ZeptoMetrix).

Electroretinogram recordings and analysis

Adult (50 days old) mice subjected to OIR and receiving Lv.shSema3A in the left eye and Lv.shGFP in the contralateral right eye were used in this study and compared with room air–raised controls. Mice were housed in the animal care facilities under a cyclic light environment (12 hours of light at 80 lux, 12 hours of dark). Electroretinogram (ERG) recordings were obtained as described previously.[21] Briefly, before the recordings, the animals were dark adapted for a period of 12 hours and anesthetized. Drops of 1% cyclopentolate hydrochloride (Alcon) were used to dilate the pupils. The animals were then placed in a chamber with a photostimulator (model PS22; Grass Instruments) and a rod-desensitizing background of 30 cd/sec/m^2. The active DTL fiber electrode (27/7 X-Static Silver coated conductive nylon yarn; Sauquoit Industries) was placed on the cornea, a reference electrode was positioned in the mouth (E5 disc electrode; Grass Instruments), and a ground electrode (E2 subdermal electrode; Grass Instruments) was inserted in the tail. Simultaneous recordings of full-field ERGs (bandwidth 1-1000 Hz, 10 000×, 6-db attenuation, P-511 amplifiers; Grass Instruments) was performed with a data acquisition system (MP 100 WS; Biopac System). Scotopic ERGs were obtained in response to progressively brighter flashes of white light ranging in intensity from −6.3 log to 0.9 log cd/s/m^2 in 0.3-log-unit increments (using a photostimulator with an interstimulus interval of 10 seconds, flash duration of 20 μs, and an average of 2-5 flashes). ERG amplitudes were measured according to a method described previously.[22] In brief, the amplitude of the a-wave was measured from baseline to trough and the b-wave from the trough of the a-wave to the highest peak of the b-wave.

Preparation of conditioned medium from hypoxic RGC-5

The RGC-5 cell line was kindly provided by Neeraj Agarwal (University of North Texas Health Science Center, Fort Worth, TX). All cells were terminally differentiated and prepared as described previously.[6] Approximately 10^6 cells were seeded before exposure to 2.0% O_2 levels. Supernatant was collected at the appropriate time points, centrifuged to remove debris, filtered with 0.2-μm filters (Millipore), and distributed for proliferation assays (see "Cell proliferation assay").

IL-1β stimulation of cultured RGC-5

Terminally differentiated RGC-5 cells (10^5/well) were seeded in 6-well plates and incubated for 0-8 hours with recombinant murine IL-1β (500 pg/mL; 211-11B; PeproTech). Cells were collected at each time point using TRIzol reagent for mRNA extraction, as described in "RT-PCR and real-time qRT-PCR."

Cell-proliferation assay

Rat brain microvascular ECs (RBMVECs) were obtained from Cedarlane Laboratories and used from passage 2-7. Cell number and division rates were determined using thymidine incorporation, in which [methyl-^{3}H]-thymidine (1 μCu/well; Amersham) was introduced to RGC-5 conditioned medium after seeding in 24-well plates. Cell proliferation was assessed after 24 hours.

Aortic explant microvascular growth assay

Aortas were explanted from adult C57BL/6 mice, sectioned into 1-mm rings, and placed into growth-factor reduced Matrigel (BD Biosciences) in 24-well plates. Rings were cultured in supplemented endothelial basal medium (Lonza) before a 40-hour exposure to RGC-5 conditioned medium. Treated rings were photographed using an inverted phase contrast microscope (Eclipse TE300; Nikon), and microvascular growth was assessed using Image Pro 4.5 software (Media Cybernetics), as described previously.[6]

Real-time migration assay

RBMVEC migration rates were assessed after exposure to the conditioned medium using a real-time cell analyzer with a dual-plate apparatus (xCELLigence RTCA DP; Roche). This migration assay provides a real-time measurement of EC migration by extrapolating changes in electrical impedance with the number of cells passing through a porous membrane. Briefly, 160 μL of complete RBMVEC medium with or without 0.5 or 1.0 μg/mL of Sema3A was loaded on the lower chamber of a cellular invasion and migration plate (CIM-Plate 16; Roche). The upper chamber was then fitted on the lower chamber and loaded with 50 μL of RBMVEC basal medium. After 1 hour of equilibration, 2.8×10^4 of RBMVECs were loaded on each well of the upper chamber. The cellular invasion and migration plate was subsequently placed on the RTCA analyzer in a 37°C incubator. The cellular migration was recorded every 15 minutes (100 sweeps at 15-minute intervals) using the cellular index provided by the manufacturer of the RTCA DP instrument (Roche). RBMVEC basal medium was used as a negative control. Four independent reactions were assayed for each condition.

Microdeposition of Sema3A

Aortic explants from adult GFP mice (see above) were plated on polycarbonate slides adjacent to microdeposited Sema3A (100 ng/μL) and vehicle controls using micropipettes. Samples were covered with growth factor-reduced Matrigel (as described in "Aortic explant microvascular growth assay"). Nascent vessels were visualized using 63× objectives with fluorescence microscopy (Eclipse E800; Nikon).

Morphometric analysis and live cell imaging

RBMVECs incubated with Sema3A and retinal ganglion cell (RGC) supernatants were photographed using a 40× air objective on a Leica DMI6000 microscope coupled to a Ultraview Vox spinning disc confocal unit (PerkinElmer). The camera was a Hamamatsu Orca-R2. Cells were maintained at 37°C using an environment chamber system from Pathology Devices. Images were acquired every 2 minutes for 45 minutes, and surface areas were calculated using ImageJ 1.40g software.

Figure 1. (continued) to vascularized areas ± SEM. **P* = .0447 compared with the vascularized zone (V). At P19, when physiologic retinal revascularization is reinstated, Sema3A in the avascular retina returns to control levels. Levels of Sema3A in the peripheral (P) and central (C) retina of normoxic controls are comparable. (D) Laser capture microdissection on retinal layers (F) (also see supplemental Figure 1B) demonstrates that Sema3A is primarily produced in the ganglion cell layer (GCL), with lower expression in the inner nuclear layer (INL). ONL indicates outer nuclear layer. Levels of Sema3A surge 4.4-fold in the GCL at P14 after OIR (n = 3). ***P* = .0075 and **P* = .0143 relative to normoxia (Norm). (E) Confocal imaging of immunohistochemistry on central avascular retinal cross-sections (OIR P14) reveals a predominant expression of Sema3A by RGCs as confirmed by merging with RGC marker Thy1.1. (G) At P17, laser capture microdissection and RT-PCR of normal vessels versus neovascular tufts revealed a 2.2-fold induction in Nrp-1 in tufts (n = 3). Values are gene copy number normalized to *CyclophilinA* standards ± SEM. ****P* = .0007 compared with controls (Ctl). (H) Immunohistochemistry on flat-mount retinas confirms pronounced staining of Nrp-1 on lectin-stained neovascular tufts (P17). Images are representative of 5 experiments. Scale bars represent 300 μm (A right panel), 500 μm (A central panel), 50 μm (A right panel) 25 μm (E), 100 μm (F), and 25 μm (H).

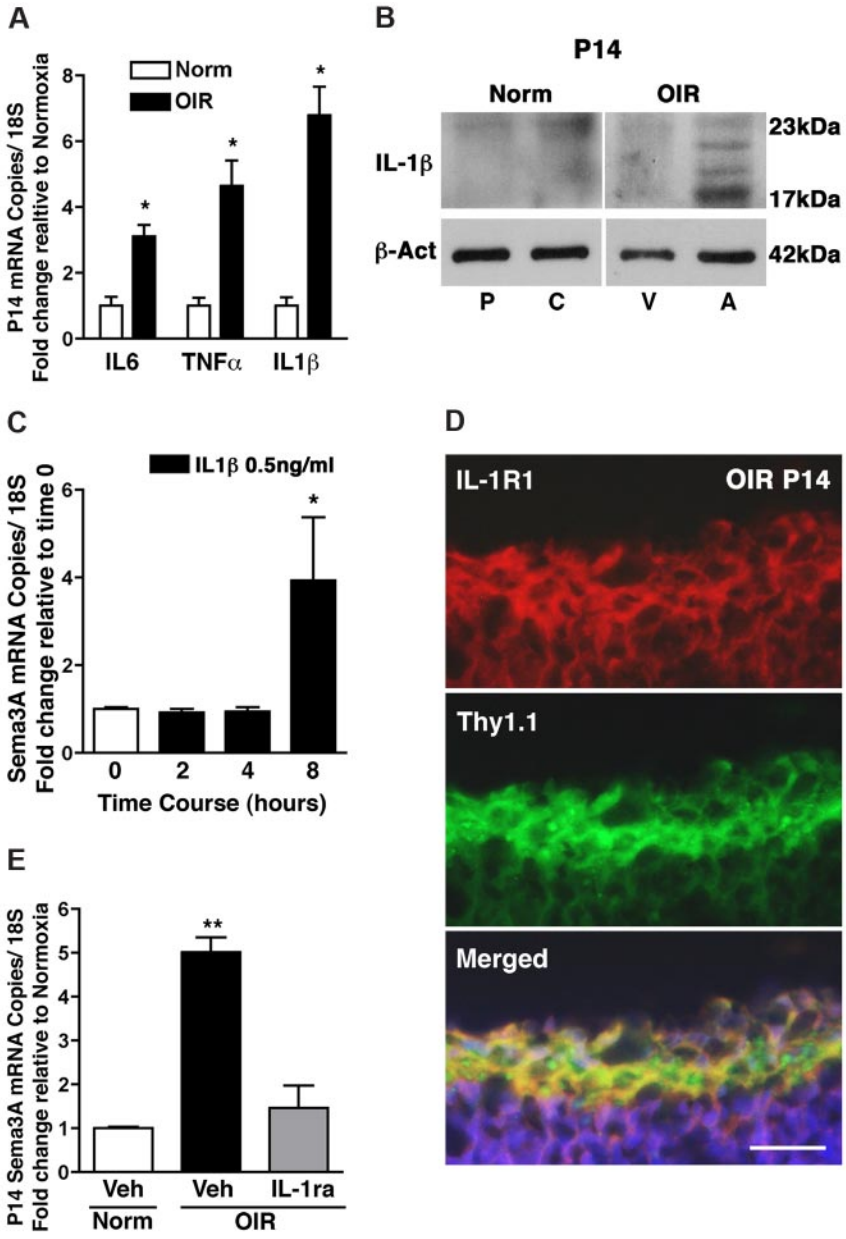

Figure 2. IL-1β in the ischemic avascular retina induces Sema3A expression. (A) The inflammatory cytokines IL-6, TNF-α, and IL-1β are induced in OIR retinas, in particular IL-1β, which was up-regulated 6.8-fold compared with normoxia. n = 3; $P < .01$ compared with normoxia (Norm). (B) Microdissection of avascular (A) regions of the OIR retina reveals a marked induction in IL-1β (17 kDa) protein levels compared with the vascular regions (V) and the central (C) and peripheral (P) normoxic retina; higher molecular weight bands correspond to pro-IL-1β. n = 3; $P < .01$ compared with time 0. (C) RGC-5 stimulated with IL-1β (0.5 ng/mL) elicited a delayed (8 hours) but significant 4-fold increase in Sema3A (n = 3-4). (D) Confocal imaging of immunohistochemistry on retinal cross-sections (OIR P14) reveals a predominant expression of IL-1RI by RGCs, as confirmed by merging with RGC marker Thy1.1. (E) IL-1RI antagonist IL-1ra (Kineret) abrogated the OIR-dependent induction of Sema3A compared with vehicle-treated normoxia and OIR controls. Values are the fold increase of control ± SEM. n = 3; $^{**}P < .01$ compared with normoxic vehicle (Veh). (D) Scale bar represents 25 μm.

Actin network visualization and RhoA pull-down

RBMVECs were incubated for 1 hour with RGC conditioned medium or Sema3A, and cells were fixed with 4% paraformaldehyde and permeabilized with 0.2% Triton X-100. Subsequently, cells were stained using rhodamine-phalloidin (0.15μM) for 30 minutes and 4′,6-diamidino-2-phenylindole, dihydrochloride (DAPI; 0.1 μg/mL) for an additional 5 minutes. Actin network collapse was assessed by confocal microscopy (LMS5; Zeiss). RhoA activity was determined using a RhoA pull-down kit (Pierce Biotechnology) according to the manufacturer's instructions. Briefly, the active RhoA (GTP-bound) fraction was isolated from 200 μg of protein lysates from RBMVECs incubated with RGC conditioned medium; 5 μg of total RhoA was used as the loading control.

Statistical analysis

Data are presented as means ± SEM. Two-tailed independent Student *t* tests was used to analyze data. Comparisons between groups were made using 1-way ANOVA followed by the post hoc Tukey multiple comparisons test among means. $P < .05$ was considered statistically significant.

Results

The expression pattern of Sema3A is temporally and geographically consistent with a role in both the vaso-obliterative and vasoproliferative phases of PR

In humans, the initial retinal vascular degeneration observed in PR yields pockets of nonperfused neuronal tissue that result in local hypoxia. Similarly, in mice, the OIR model (75% oxygen from P7-P12 and room air until P17) provokes a central avascular retinal region (Figure 1A left and center panels). As the retina revascularizes, aberrant neovascularization peaks at P17[3,23] (supplemental Figure 1, available on the *Blood* Web site; see the Supplemental Materials link at the top of the online article), when vascular tufts protruding into the vitreous are found bordering the avascular zone (Figure 1A right and center panels). In accordance with a role in retinopathy, Sema3A levels in whole retina (as determined by

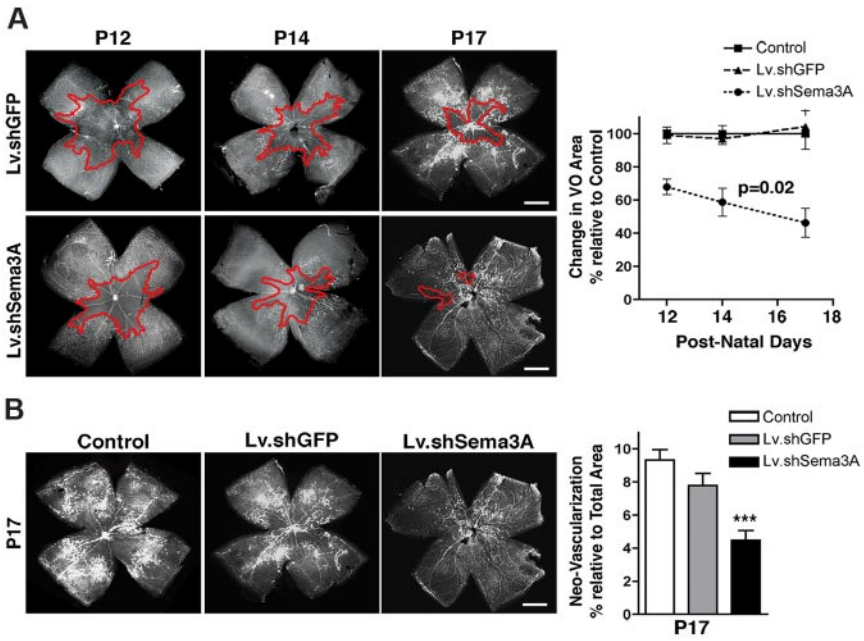

Figure 3. RGC-derived Sema3A partakes in vaso-obliteration, hinders vascular regeneration, and contributes to preretinal neovascularization in OIR. (A) Representative photomicrographs of *Griffonia simplicifolia* lectin-stained flat-mount retinas at P12 reveal that mice receiving an intravitreal injection of Lv.shSema3A show a 32% reduction in the area of vaso-obliteration compared with contralateral eyes receiving Lv.shGFP injections and noninjected eyes (basal) revealing the vasotoxic properties of Sema3A in the first phase of OIR (n = 13-15; additional quantification is presented in supplemental Figure 4A). The inhibition of RGC-derived Sema3A significantly enhanced the rate of vascular regeneration secondary to OIR as determined at P12 (n = 13-15), P14 (n = 12-13), and P17 (n = 15-18). Values are presented as the rate change in vaso-obliterated areas relative to Lv.shGFP-treated controls ± SEM. $P = .02$ by ANOVA factoring for time and group. (B) At peak neovascularization (P17) lectin-stained flat-mount retinas reveal that inhibition of Sema3A (n = 9-12) significantly reduced areas of pathologic neovascularization from 9.3% to 4.5%, as determined using the SWIFT-NV quantification protocol (supplemental Figure 4B). Values are presented as areas of neovascularization relative to total retinal area ± SEM. ***$P = .0002$ compared with control. Scale bars in panels A and B represent 500 μm.

RT-PCR) surge 3-fold ($P = .0015$) during the height of vascular obliteration immediately after exposure to high O_2 concentrations at P8, and persist during pre–retinal neovascularization formation at P14 ($P = .0157$; Figure 1B). At P14, when pre–retinal neovascularization commences (supplemental Figure 1), this increase in Sema3A is precisely located to central avascular zones in microdissected retinas (Figure 1C). Although VEGF levels significantly increase in this avascular zone (supplemental Figure 2), nascent vessels fail to enter. Moreover, Sema3A mRNA expression (by RT-PCR) was markedly increased in OIR in the ganglion cell layer (Figure 1D; $P = .0075$) as isolated by laser capture microdissection (Figure 1F), whereas less expression was noted in the inner nuclear layer (Figure 1D). These findings were confirmed by immunohistochemical localization of Sema3A in the ganglion cell layer of the central avascular retina in OIR (P14), specifically in RGCs expressing Thy1.1 (Figure 1E). At P19, when physiologic revascularization progresses after the earlier peak of neovascularization (supplemental Figure 1),[15-17] Sema3A levels decreased in the central avascular zones to values detected at the periphery (Figure 1C), which is consistent with a revascularization of the retina (supplemental Figure 1). Bordering the Sema3A-rich avascular retina, Nrp-1 expression was increased in pathologic pre-retinal vascular tufts. In contrast to Sema3A, which was mainly found within the avascular zone, Nrp-1 was increased in pre-retinal vascular tufts (P17; supplemental Figure 1B) that are present in the periphery of this central avascular zone (Figure 1G-H). These data suggest that Sema3A generated by RGCs is induced during the vaso-obliterative phase of PR and is positioned to block subsequent desirable revascularization during the proliferative phase (Figure 7C).

IL-1β in the ischemic core of the retina induces Sema3A expression

During vascular injury, the neural retina mounts an inflammatory response to the insult. Accordingly, levels of various cytokines such as IL-1β,[24,25] IL-6,[25-27] and TNF-α[7,28] are increased in the vitreous fluid of patients with diabetic PR, in the retinas of diabetic rats, and during the proliferative phase of retinopathy of prematurity. We determined whether the induction of Sema3A in the ischemic core of the retina was dependent on inflammation. Retinal levels of the key inflammatory mediators IL-6, TNF-α, and IL-1β were increased at P14 in OIR (Figure 2A; $P < .05$). Although cytokine signaling is interrelated, we focused on IL-1β, which was markedly elevated and largely confined to the avascular retina (Figure 2B) in regions of elevated Sema3A expression (Figure 1C). Stimulation of IL-1RI–expressing RGCs (supplemental Figure 3A) with IL-1β induced a robust rise in Sema3A expression (Figure 2C). The induction of Sema3A was only noted after prolonged exposure to IL-1β (starting at 8 hours), and therefore suggests that a sustained inflammatory stress is required to trigger the production of this cue. Concordant with RGCs being the main source of Sema3A, we localized IL-1RI in this neuronal population in retinal cross-sections (Figure 2D) and in retinal astrocytes (supplemental Figure 3B). To ascertain the role of the inflammatory stimulus, specifically IL-1β, in the generation of Sema3A in OIR, we determined the effects of an IL-1 receptor antagonist (IL-1ra; Kineret) on Sema3A expression. IL-1ra administered twice daily starting at P10 fully inhibited the production of Sema3A in OIR at P14 (Figure 2E), further confirming a role for inflammatory stress in governing the expression of this repulsive cue.

RGC-derived Sema3A partakes in vaso-obliteration, hinders vascular regeneration, and contributes to pre-retinal neovascularization in OIR

Physiologic and pathologic retinal vascularization is orchestrated by the coordinated interplay of ECs, astrocytes, microglia,[2,29,30] and neurons such as RGCs.[3] Given the pivotal role of the latter in retinal vascular homeostasis[3] and the relative abundant expression of Sema3A in RGCs (Figure 1D-E), we proceeded to knock down Sema3A mRNA in these neurons using shRNA encoded in lentivectors (Lv); this approach was favored over the use of Sema3A transgenic mice, which exhibit high mortality rates and confounding neuronal deficits.[31] Surviving Sema3A transgenic pups are also small for gestational age,[32] which would independently alter their OIR phenotype.[20] Intraocular injection of Lv at P2 effectively infected ~ 70% of RGCs, as determined 72 hours after

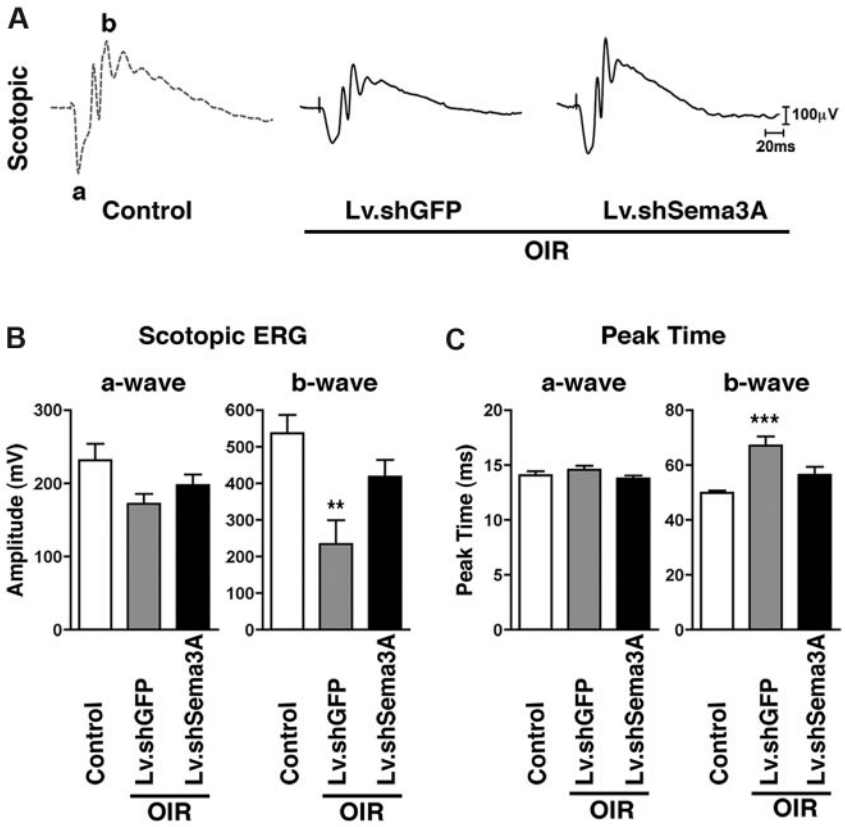

Figure 4. Inhibition of RGC-derived Sema3A during PR preserves neuroretinal function. (A) Representative recordings of full-field scotopic ERGs in response to progressively brighter flashes of white light ranging in intensity from −6.3 to 0.9 log cd/s/m^2 in 0.3 log-unit increments (using a photostimulator with an interstimulus interval of 10 seconds, flash duration of 20 μs, and an average of 2-5 flashes). (B) Lv.shSema3A-treated mice show a significant gain in inner-retinal scotopic (mixed cone-rod) b-wave response (418.2 μV; n = 6) compared with control contra-lateral Lv.shGFP μV (234.3; n = 8) injected eyes. $^{**}P < .01$ and $^{***}P < .001$ compared with corresponding controls. Similarly, knockdown of Sema3A enhances the response time to light stimulus, as illustrated by decreased peak times (56.4 ms) with respect to controls (67.1 ms). Inner retinal function as determined by a-wave amplitudes and peak times was not significantly affected.

infection[3] (GFP colocalization with the RGC marker Thy1.1; supplemental Figure 4A) and led to a ~ 50% reduction ($P < .05$) in retinal Sema3A, whereas the Sema3A levels in contralateral control eyes infected with Lv.shGFP were unaffected (supplemental Figure 4B-C). The expression of related semaphorins and VEGF remained unaltered, confirming the specificity of the Lv.shSema3A (supplemental Figure 4C-D).

Mice injected with Lv.shSema3A exhibited 32% less O_2-induced vaso-obliteration at P12, which is consistent with Sema3A's proapoptotic properties in ECs[33] ($P < .01$) (Figure 3A and supplemental Figure 5A). Moreover, before and during the vasoproliferative phase (P12-P17), revascularization of the central avascular zone was accelerated by 3.7-fold in animals treated with Lv.shSema3A ($P = .02$ linear regression; Figure 3A). More rapid restoration of retinal vasculature was associated with less preretinal neovascularization (Figure 3B and supplemental Figure 5B), as expected.[23,34,35] These findings introduce a new neurovascular paradigm in which stressed neurons express Sema3A and contribute to promoting the degeneration of the surrounding vasculature, which deviates nascent vessels away from the most severely ischemic areas in an attempt to redistribute metabolic resources to areas deemed "more salvageable."[36]

Inhibition of RGC-derived Sema3A during PR preserves neuroretinal function

Maintaining neural function in ischemic tissue requires preservation of the local vascular supply. Accelerated postischemic revascularization is associated with improved neural recovery.[37,38] OIR is associated with sustained depression in retinal function,[39] primarily in the inner retina (as reflected by the b-wave amplitude of the ERG).[5] To assess the functional benefits of inhibition of RGC-derived Sema3A, we performed short-flash ERG analysis in 50-day-old OIR mice. We found that suppression of Sema3A (using Lv.shSema3A) in animals subjected to OIR preserves inner neuroretinal function, as demonstrated by enhanced scotopic (mixed cone-rod) b-wave amplitudes compared with Lv.shGFP-injected controls ($P = .0049$; Figure 4A-B). This Lv.shSema3A-induced improvement in amplitude was accompanied by renormalization of the delayed b-wave peak times ($P = .001$; Figure 4C). Outer retinal function, as determined by a-wave amplitudes, was not significantly affected (Figure 4B).

Sustained hypoxia in RGCs induces Sema3A and blocks EC growth

Given the inferred neurovascular cross-talk observed, we sought to decipher the cellular dynamics governing Sema3A expression and actions. We first explored Sema3A production using an in vitro model of RGCs[40] exposed to hypoxia (2% O_2).[3] As expected, in response to hypoxia, VEGF mRNA increased promptly (within 6 hours; Figure 5A), which is consistent with the initial attempt of VEGF to protect ischemic neurons and promote vascular regrowth. This was confirmed by increased proliferation of RBMVECs and vascular sprouting of aortic explants exposed to 12 hours of hypoxia in RGC medium; the addition of rSema3A (800 ng/mL) to this VEGF-rich medium abolished its proliferative effect (Figure 5B-C). By 24 hours of hypoxia, VEGF levels subsided, followed at 36 and 48 hours by sharp increases in Sema3A mRNA ($P < .0001$; Figure 5A), which is in agreement with hypoxia- and/or oxidant stress–induced regulation of other semaphorins.[41] Accordingly, conditioned medium from hypoxic RGCs taken at 40 hours reduced basal RBMVEC division by 70% (suggestive of cell death; $P < .01$), as well as vessel sprouting from aortic explants (Figure

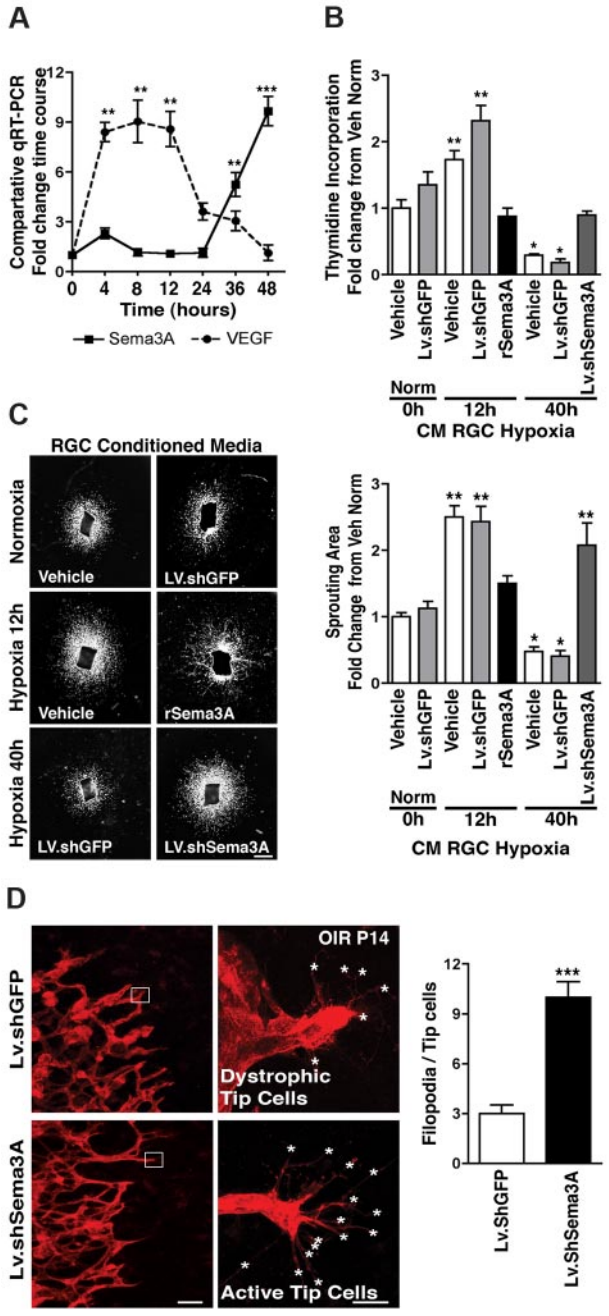

Figure 5. Sema3A produced by hypoxic RGCs prevents retinal EC growth. (A) VEGF and Sema3A release by cultured RGC-5 cells exposed to hypoxia (2%). In the initial 12 hours after hypoxia, VEGF levels rapidly rise ~ 9-fold, whereas Sema3A remains unaffected. Later, as hypoxic exposure is prolonged, Sema3A levels rise (6-fold at 36 hours and 10-fold at 48 hours). Values represent the fold increase relative to time 0. $^{**}P < .01$ and $^{***}P < .0001$ compared with corresponding time 0. (B) Neuromicrovascular EC proliferation as measured by thymidine incorporation. Incubation of ECs with conditioned medium from RGCs exposed to hypoxia for 12 hours (high VEGF, low Sema3A) caused a 1.7-fold (vehicle) and 2.3-fold (nonspecific shRNA; LV.shGFP) increase in cell number within 24 hours; this effect was abrogated by rSema3A (800 ng/mL). Conversely, ECs treated with conditioned medium from RGCs exposed to hypoxia for 40 hours (low VEGF, high Sema3A), showed a Sema3A-dependent reduction in EC division (5-fold diminution). Knockdown of Sema3A in hypoxia-exposed RGCs using Lv.shSema3A prevented the decrease in EC division compared with vehicle- and Lv.shGFP-treated RGCs. n = 4-6; $^{*}P < .05$ and $^{**}P < .01$ compared with vehicle during normoxia (Norm) at time 0. (C) Aortic sprouting more than doubled in explants grown in conditioned medium from vehicle- and LV.shGFP-treated RGCs exposed to 12 hours of hypoxia; this vascular growth was curbed by rSema3A (800 ng/mL). Conditioned medium from RGCs exposed to 40 hours of hypoxia reduced their sprouting by ~ 60% compared with normoxic medium controls. When Sema3A was knocked down in RGCs, vascular sprouting was doubled compared with Lv.shGFP, underscoring the inhibitory properties of Sema3A toward nascent vessels. Values are represented as the fold change relative to controls. n = 3-6; $^{*}P < .05$ and $^{**}P < .01$ compared with vehicle during normoxia (Norm) at time 0. (D) Representative confocal images of the revascularization front (images on left) and high magnification of tip cells (images on right) at OIR P14. The number of filopodia (asterisks) per tip cell was increased 3-fold in Lv.shSema3A animals, whereas contralateral eyes treated with Lv.shGFP showed fewer filopodia and dystrophic tip cells. n = 10; $^{***}P < .0001$ compared with value for Lv.shGFP. Scale bars represent 1 mm (C), 50 μm (D left), and 10 μm (D right).

5B-C). These effects were abolished by Sema3A knockdown in the hypoxic RGCs using Lv.shSema3A (~95% infection efficiency and 50% knockdown; supplemental Figure 6A) compared with Lv.shGFP controls. Our findings reveal that Sema3A is produced by hypoxic stress–injured neurons and support our hypothesis that these injured RGCs participate in hindering revascularization of ischemic retinal tissue.

Revascularization of ischemic tissues begins with the selection at the vascular front of highly motile ECs known as tip cells, which express several chemosensitive receptors (eg, Sema3A-responsive Nrp1) and are believed to follow guidance and growth cues with their elaborate filopodial extensions.[10] Accordingly, in control (as well as in Lv.shGFP-treated) mice subjected to OIR, tip cells at the retinal vascular front bordering the avascular zone rich in Sema3A exhibited mostly short and dystrophic filopodia (Figure 5D). Conversely, in mice with RGC knockdown of Sema3A, vascular filopodia were 3-fold more abundant (Figure 5D). These data underscore the role of neuron-derived Sema3A in stalling vascular regeneration of ischemic tissues.

RGC-derived Sema3A repels nascent vessels

Aberrant vessel guidance as an etiology of disease has thus far not been considered. Although Sema3A has been reported to affect EC motility,[9] its role in guiding vessels remains elusive. We corroborated this influence on cell motility in a real-time migration assay, demonstrating that hypoxic RGCs produce sufficient Sema3A to significantly impede EC movement and thus reduce rates of migration ($P < .05$; Figure 6A). The effect of Sema3A in specifically deviating vessels was also observed, because nascent vessels (from aortic explants of germline-GFP mice) steered away from microdeposited Sema3A (Figure 6B-C).

Steering endothelial tip cells toward the desired trajectories requires dynamic cytoskeletal rearrangement involving actin polymerization, the formation of stress fibers, and focal adhesion points, which together modulate cytoplasmic morphology and are required to instigate movement. In agreement with this, RGC-derived Sema3A influences EC shape. Conditioned medium from hypoxic RGCs (40 hours) caused rapid EC deformation (assessed using live spinning-disk imaging) (Figure 6D) to a similar extent as that observed with rSema3A (Figure 6E and supplemental Figure 6B). The effects on cell shape and motility translate into a loss of stress fibers (as determined by F-actin staining with rhodamine-phalloidin) by hypoxia-inducing Sema3A (Figure 6F); these changes are abrogated by Sema3A knockdown in RGCs (Figure 6D and 6F).

Actin alignment, cell shape, and stress fiber formation are under the control of small GTPases such as RhoA, which activate Rho kinase, leading to myosin light-chain phosphorylation and contributing to actomyosin contraction and cell motility. In agreement with the promotion of tip cell formation and subsequent growth of vessels, conditioned medium from RGCs silenced of Sema3A promoted RhoA activation in ECs (as determined by RhoA-GTP

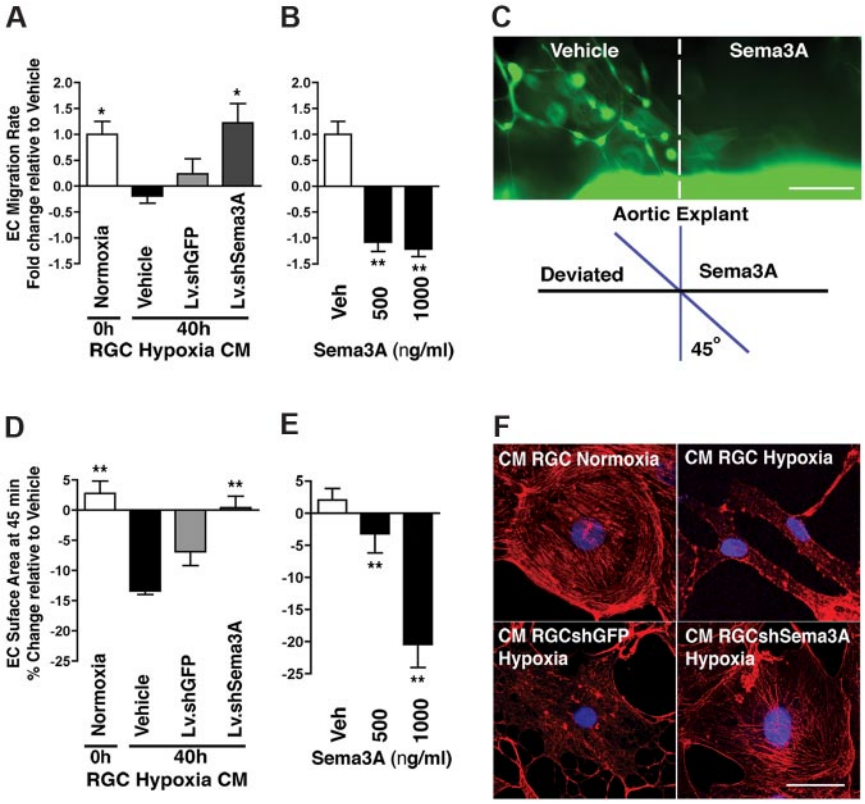

Figure 6. Sema3A produced by hypoxic RGCs repels nascent vessels. (A) Rates of RBMEC migration using a real-time cell analyzer. EC motility was significantly blocked by hypoxia-induced Sema3A (4.2-fold) and rescued by conditioned medium from hypoxic RGC in which Sema3A was silenced (40 hours). n = 4; $^{*}P < .05$ compared with vehicle at 40 hours of hypoxia. (B) Effect of rSema3A on EC migration rate (over 45 minutes). n = 3; $^{**}P < .01$ compared with vehicle (Veh). (C) Propensity of Sema3A to deviate (repel) nascent vessels was established using microdeposited Sema3A adjacent to aortic explants from GFP mice. Vascular sprouts invaded vehicle-coated regions but avoided Sema3A-coated zones. (D) RGC-derived Sema3A modulates EC cytoskeletal arrangements and morphology, as demonstrated by time-lapse morphometric analysis of RBMECs subjected to conditioned medium (supplemental Figure 6B). ECs exposed for 45 minutes to conditioned medium from hypoxic RGCs (40 hours) contracted, whereas knockdown of Sema3A in the RGCs largely abrogated this effect. n = 3; $^{**}P < .01$ compared with vehicle at 40 hours of hypoxia. (E) rSema3A provoked a dose-dependent cellular contraction (22.5%), similar in magnitude to 40 hours of hypoxic conditioned medium. n = 3; $^{**}P < .01$ compared with vehicle (Veh). (F) Actin stress fibers in ECs. Treatment of ECs with hypoxic conditioned medium from hypoxic retinas resulted in loss of actin stress fibers and collapse of the actin network (as determined by rhodamine-phalloidin staining [red]); knockdown of Sema3A in RGCs abrogated this effect. Therefore, changes in actin are consistent with those on cell shape and movement (panels A-E). Images are representative of 4 experiments. Nuclei are stained with 4′,6-diamidino-2-phenylindole, dihydrochloride (blue). Scale bars represent 20 μm (C) and 50 μm (F).

pull-down; supplemental Figure 6C). These findings are consistent with changes in EC migration affected by Sema3A (Figure 6A-C) and by the tip cell phenotype observed at the vascular front of OIR mice (Figure 5D).

The source of Sema3A release dictates the direction of the repulsive and anti-angiogenic force acting on tip cells. In OIR (as presented in Figure 1), Sema3A was produced by ischemic RGCs of the avascular zone under the superficial retinal vascular layer (Figure 7A), causing neovessels to steer away from the central zone toward the vitreous to form pathologic vascular tufts. Intravitreal injections of rSema3A (into the pre-retinal vitreous) after OIR (P14) prevented the entry of neovessels in the vitreous body and thus decreased vascular tuft formation at P17 (Figure 7B). Although a trend was noted, vaso-obliteration in rSema3A-treated retinas also tended to decrease, albeit not significantly (Figure 7B). Our data suggest that regional production of Sema3A by markedly hypoxic RGCs participates in deviating neovessels away from the avascular ischemic retina, thus hindering functional revascularization of avascular retinal zones, as depicted in the schematic diagram in Figure 7C.

Discussion

Neuronal metabolism is tightly coupled to vascular supply by regulating vasomotoricity and in a more sustained manner through the release of several growth factors.[3] However, the reasons that vessels fail to invade distinct zones of ischemic yet salvageable neural tissue are to date poorly understood. This study provides the first proof of concept for a neuronal factor implicated in microvascular degeneration, and identifies neuronally derived Sema3A as a vascular repulsive cue that also actively participates in mediating the key features of PRs. Paradoxically, our findings show that hypoxic ischemia causes neurons to reverse their signaling machinery from VEGF production to the expression of the vascular chemorepellent and the cytotoxic cue Sema3A at the expense of VEGF (Figure 5A). This sacrifice of injured neurons could be a mechanism to preserve the integrity of the remaining neurovascular network by shunting revascularization away from irreversibly damaged tissue (sustained loss of inner retinal function). In doing so, neurons mount a chemical barrier that deviates neovessels, isolating the damaged retina away from healthy regions. This novel mechanism involving Sema3A also provides an alternative explanation for the pathognomonic phenotype of ridge and tuft formation observed in ischemic PRs.

The factors that regulate expression of Sema3A remain elusive. Although general hypoxia and/or oxidant stress have been shown to affect other semaphorins,[41,42] our study is the first to draw a direct link between the inflammatory stress present in ischemic neural tissue and the induction of semaphorins. Consistent with the theory of segregating damaged areas of tissue, the induction of Sema3A requires prolonged exposure to inflammatory cytokines (here notably IL-1β), a scenario akin to prolonged exposure to damaging ischemia. Our findings thus expose a new pathophysiologic role for neuronally derived Sema3A that extends beyond its previously reported antiangiogenic properties.

The paradigm presented herein may also apply to other areas of the eye and the central nervous system. Increased levels of repulsive guidance cues (including Sema3A) are released from choroidal neovascular retinal pigmented epithelium.[43] Guidance cues may therefore also contribute to diseases of the outer retina, such as age-related macular degeneration. Shortly after an ischemic stroke,[44] Sema3A is produced by injured cells[45,46] and localizes to regions immediately adjacent to the infarct.[46] A similar pattern is observed after spinal cord injury, when neurons near the site of lesion increase production of Sema3A.[47] The timing of this

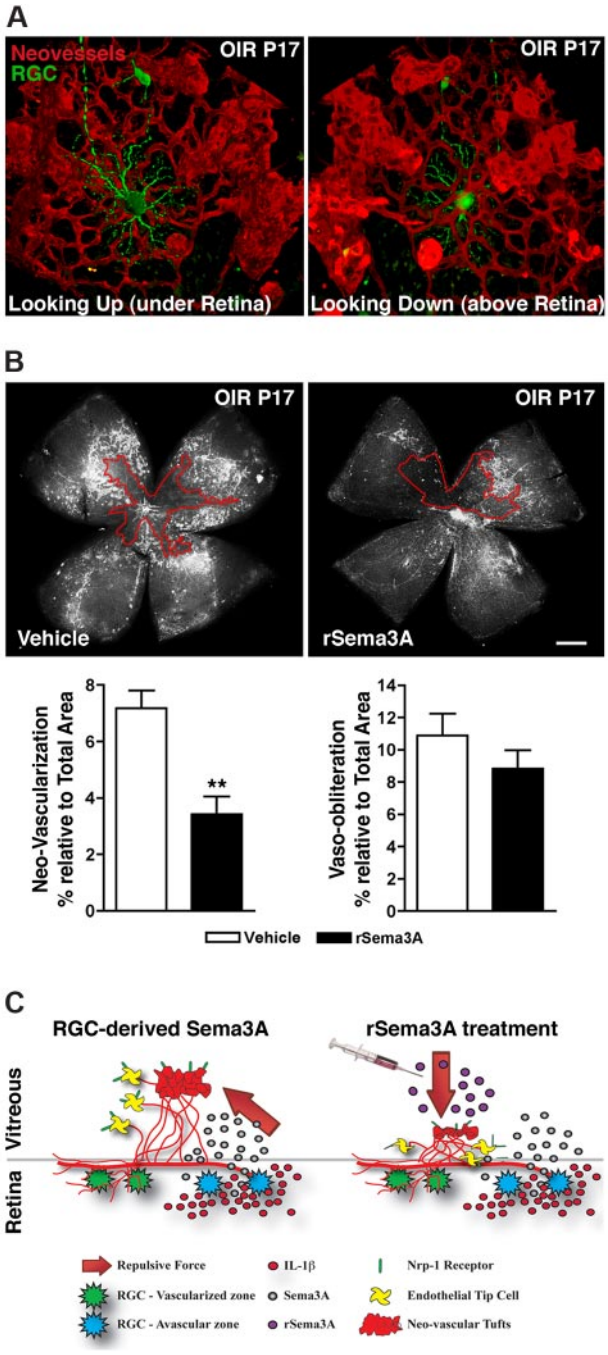

Figure 7. Intravitreal delivery of rSema3A suppresses pre-retinal neovascularization in OIR. (A) 3D reconstructions of pathologic neo-vessels and RGC-YFP at P17 after OIR. The spatial distribution of retinal neurons and vessels results in the repulsion of neovascular tufts toward the vitreous. (B) Intravitreal injection of rSema3A (100 ng; P14) halved the formation of preretinal vascular tufts at P17. n = 7; $^{**}P = .0012$ compared with corresponding vehicle. (C) Schematic summary illustrates ischemic neurons in the avascular zones, producing Sema3A secondary to inflammatory stress (IL-1β). Pathologic neovascular tufts are enriched in Nrp-1. RGC-derived Sema3A impedes revascularization and repels neo-vessels away from the avascular neural retina toward the vitreous (left), whereas intravitreal rSema3A (injected) prevents preretinal invasion of pathologic neovessels (right).

increase corresponds to the early phases of the response to injury when vascular remodeling occurs and axonal sprouting is induced. However, in addition to the direct effects of repulsive cues such as semaphorins on cellular proliferation in models of tumorigenesis,[48,49] the involvement of guidance cues in pathologic settings has not been explored previously. In light of the ubiquitous release of Sema3A by injured neurons elsewhere in the central nervous system, the present study suggests that modulation of this guidance cue could be harnessed as a therapeutic strategy to promote prompt revascularization of ischemic neural tissue.

In agreement with our current mechanistic understanding of PRs, VEGF has been the most promising therapeutic target for ocular vasoproliferative diseases, albeit with concerns. Notwithstanding the contribution of excessive levels of VEGF in PRs, this growth factor also plays a pivotal protective role in the normal physiologic development and health of the retina.[50,51] Inhibiting VEGF may curb neovascularization, but may also cause unwanted damage to neuronal networks; accordingly, the appropriate dose of anti-VEGF treatment remains a challenge.[52] Alternatively, inhibiting the repulsive forces that are only present during a pathologic insult may prove to be a more selective therapeutic approach.

Although the mechanisms governing vascular degeneration and the ensuing pre-retinal neovascularization in PRs have been studied,[13,53-57] there are currently no strategies to accelerate revascularization of the vaso-obliterated area and consequently limit aberrant pre-retinal neovascularization. We propose that inhibition of neuronally derived Sema3A aids the physiologic vascular regeneration of the retina by overriding the vaso-inhibitory status of the injured tissue, thus alleviating the hypoxic stress that is central to disease progression. Accordingly, inhibition of RGC-derived Sema3A or upstream inflammatory mediators (notably IL-1β), while harnessing the growth potential of VEGF (supplemental Figures 2 and 4), may also force vessels to promptly revascularize injured neurons and improve retinal function. rSema3A may also curb pathologic neovascularization; however, as is the case with anti-VEGF therapy, this approach would curtail beneficial rapid retinal revascularization.[7] Therefore, the modulation of RGC-derived Sema3A may be a preferable therapeutic modality to remedy PRs without directly sequestering growth factors such as VEGF that are essential for endothelial and neuronal homeostasis. Because Sema3A is also released by injured neurons elsewhere in the central nervous system,[9,46,47] the concept proposed herein may not only apply to ischemic retinopathies, but also to other pathologies such as cerebral infarct, in which vascular growth is a key determinant of outcome.[37,38]

Acknowledgments

We thank Dr Montoya-Zavala for expert advice on guidance assays.

J.-S.J. is a recipient of the Canadian Child Health Clinician Scientist Program, a Canadian Institute of Health Research (CIHR) training initiative; N.S. is supported by a Frederick-Banting scholarship from the CIHR; F.B. holds a Fonds de la Recherche en Santé du Quebec (FRSQ) fellowship; J.-C.R. is supported by the Heart and Stroke Foundation of Canada (HSCF) and the Canadian Stroke Network (CSN); L.E.H.S. is supported by the National Institutes of Health (EY017017, EY017017-04S1, P01 HD18655), by a Research to Prevent Blindness (RPB) Senior Investigator Award, by the Lowy Medical Institute (MacTel), by the Rosche Foundation for Anemia Research, and by the V. Kann Rasmussen Foundation; S.C. holds a Canada Research Chair (Translational Research in Vision) and the Leopoldine Wolfe Chair in translational research in age-related macular degeneration and is supported by grants from the CIHR; and P.S. holds a Canada Research Chair in Retinal Cell Biology and is supported by grants from the

CIHR and the Canadian National Institute for the Blind and the Maisonneuve-Rosemont Hospital Foundation.

J.S.J. and N.S. are doctoral candidates at McGill University and Université de Montréal, respectively. This work was submitted in partial fulfillment of the requirement for the doctorate.

Authorship

Contribution: J.-S.J., N.S., S. Chemtob, and P.S. conceived and designed the experiments; J.-S.J., N.S., F.B., J.-C.R., A.S., K.Z., Z.S., A.P., T.Z., D.H., M.D., D.K., J.-C.H., E.P., A.Z., G.H., S. Costantino, C.B., and P.S. performed experiments; D.R.V., G.H., J.M., M.K., S. Costantino, C.B., P.L., and L.E.H.S. provided expert advice; M.K. and C.B. provided gene expression vectors; all authors analyzed the data; and J.-S.J., N.S., S. Chemtob, and P.S. wrote the manuscript.

Conflict-of-interest declaration: The authors declare no competing financial interests.

Correspondence: Przemyslaw (Mike) Sapieha, PhD, or Sylvain Chemtob, MD, PhD, Maisonneuve-Rosemont Hospital Research Centre, and CHU Ste-Justine, Research Centre 5415 Assomption Blvd, Montreal, Quebec, H1T 2M4, Canada; e-mail: Mike.Sapieha@umontreal.ca or Sylvain.Chemtob@umontreal.ca.

References

1. Sapieha P, Joyal J-S, Rivera JC, et al. Retinopathy of prematurity: understanding ischemic retinal vasculopathies at an extreme of life. *J Clin Invest.* 2010;120(9):3022-3032.
2. Stone J, Itin A, Alon T, et al. Development of retinal vasculature is mediated by hypoxia-induced vascular endothelial growth factor (VEGF) expression by neuroglia. *J Neurosci.* 1995;15(7 Pt 1):4738-4747.
3. Sapieha P, Sirinyan M, Hamel D, et al. The succinate receptor GPR91 in neurons has a major role in retinal angiogenesis. *Nat Med.* 2008;14(10):1067-1076.
4. Dorfman A, Dembinska O, Chemtob S, Lachapelle P. Early manifestations of postnatal hyperoxia on the retinal structure and function of the neonatal rat. *Invest Ophthalmol Vis Sci.* 2008;49(1):458-466.
5. Dorfman AL, Polosa A, Joly S, Chemtob S, Lachapelle P. Functional and structural changes resulting from strain differences in the rat model of oxygen-induced retinopathy. *Invest Ophthalmol Vis Sci.* 2009;50(5):2436-2450.
6. Sapieha P, Hamel D, Shao Z, et al. Proliferative retinopathies: angiogenesis that blinds. *Int J Biochem Cell Biol.* 2010;42(1):5-12.
7. Stahl A, Sapieha P, Connor KM, et al. Short communication: PPAR gamma mediates a direct antiangiogenic effect of omega 3-PUFAs in proliferative retinopathy. *Circ Res.* 2010;107(4):495-500.
8. Carmeliet P, Tessier-Lavigne M. Common mechanisms of nerve and blood vessel wiring. *Nature.* 2005;436(7048):193-200.
9. Miao HQ, Soker S, Feiner L, Alonso JL, Raper JA, Klagsbrun M. Neuropilin-1 mediates collapsin-1/semaphorin III inhibition of endothelial cell motility: functional competition of collapsin-1 and vascular endothelial growth factor-165. *J Cell Biol.* 1999;146(1):233-242.
10. Klagsbrun M, Eichmann A. A role for axon guidance receptors and ligands in blood vessel development and tumor angiogenesis. *Cytokine Growth Factor Rev.* 2005;16(4-5):535-548.
11. Klagsbrun M, Takashima S, Mamluk R. The role of neuropilin in vascular and tumor biology. *Adv Exp Med Biol.* 2002;515:33-48.
12. Mamluk R, Gechtman Z, Kutcher ME, Gasiunas N, Gallagher J, Klagsbrun M. Neuropilin-1 binds vascular endothelial growth factor 165, placenta growth factor-2, and heparin via its b1b2 domain. *J Biol Chem.* 2002;277(27):24818-24825.
13. Serini G, Valdembri D, Zanivan S, et al. Class 3 semaphorins control vascular morphogenesis by inhibiting function. *Nature.* 2003;424(6947):391-397.
14. Maione F, Molla F, Meda C, et al. Semaphorin 3A is an endogenous angiogenesis inhibitor that blocks tumor growth and normalizes tumor vasculature in transgenic mouse models. *J Clin Invest.* 2009;119(11):3356-3372.
15. Smith LE, Wesolowski E, McLellan A, et al. Oxygen-induced retinopathy in the mouse. *Invest Ophthalmol Vis Sci.* 1994;35(1):101-111.
16. Aiello LP, Pierce EA, Foley ED, et al. Suppression of retinal neovascularization in vivo by inhibition of vascular endothelial growth factor (VEGF) using soluble VEGF-receptor chimeric proteins. *Proc Natl Acad Sci U S A.* 1995;92(23):10457-10461.
17. Stahl A, Connor KM, Sapieha P, et al. The mouse retina as an angiogenesis model. *Invest Ophthalmol Vis Sci.* 2010;51(6):2813-2826.
18. Connor KM, Krah NM, Dennison RJ, et al. Quantification of oxygen-induced retinopathy in the mouse: a model of vessel loss, vessel regrowth and pathological angiogenesis. *Nat Protoc.* 2009;4(11):1565-1573.
19. Stahl A, Connor KM, Sapieha P, et al. Computer-aided quantification of retinal neovascularization. *Angiogenesis.* 2009;12(3):297-301.
20. Stahl A, Chen J, Sapieha P, et al. Postnatal weight gain modifies severity and functional outcome of oxygen-induced proliferative retinopathy. *Am J Pathol.* 2010;177(6):2715-2723.
21. Cayouette M, Behn D, Sendtner M, Lachapelle P, Gravel C. Intraocular gene transfer of ciliary neurotrophic factor prevents death and increases responsiveness of rod photoreceptors in the retinal degeneration slow mouse. *J Neurosci.* 1998;18(22):9282-9293.
22. Marmor MF, Fulton AB, Holder GE, Miyake Y, Brigell M, Bach M. ISCEV Standard for full-field clinical electroretinography (2008 update). *Doc Ophthalmol.* 2009;118(1):69-77.
23. Connor KM, SanGiovanni JP, Lofqvist C, et al. Increased dietary intake of omega-3-polyunsaturated fatty acids reduces pathological retinal angiogenesis. *Nat Med.* 2007;13(7):868-873.
24. Abu el Asrar AM, Maimone D, Morse PH, Gregory S, Reder AT. Cytokines in the vitreous of patients with proliferative diabetic retinopathy. *Am J Ophthalmol.* 1992;114(6):731-736.
25. Carmo A, Cunha-Vaz JG, Carvalho AP, Lopes MC. L-arginine transport in retinas from streptozotocin diabetic rats: correlation with the level of IL-1 beta and NO synthase activity. *Vision Res.* 1999;39(23):3817-3823.
26. Funatsu H, Yamashita H, Shimizu E, Kojima R, Hori S. Relationship between vascular endothelial growth factor and interleukin-6 in diabetic retinopathy. *Retina.* 2001;21(5):469-477.
27. Canataroglu H, Varinli I, Ozcan AA, Canataroglu A, Doran F, Varinli S. Interleukin (IL)-6, interleukin (IL)-8 levels and cellular composition of the vitreous humor in proliferative diabetic retinopathy, proliferative vitreoretinopathy, and traumatic proliferative vitreoretinopathy. *Ocul Immunol Inflamm.* 2005;13(5):375-381.
28. Limb GA, Chignell AH, Green W, LeRoy F, Dumonde DC. Distribution of TNF alpha and its reactive vascular adhesion molecules in fibrovascular membranes of proliferative diabetic retinopathy. *Br J Ophthalmol.* 1996;80(2):168-173.
29. Checchin D, Sennlaub F, Levavasseur E, Leduc M, Chemtob S. Potential role of microglia in retinal blood vessel formation. *Invest Ophthalmol Vis Sci.* 2006;47(8):3595-3602.
30. Fruttiger M, Calver AR, Kruger WH, et al. PDGF mediates a neuron-astrocyte interaction in the developing retina. *Neuron.* 1996;17(6):1117-1131.
31. Behar O, Golden JA, Mashimo H, Schoen FJ, Fishman MC. Semaphorin III is needed for normal patterning and growth of nerves, bones and heart. *Nature.* 1996;383(6600):525-528.
32. Gu C, Rodriguez ER, Reimert DV, et al. Neuropilin-1 conveys semaphorin and VEGF signaling during neural and cardiovascular development. *Dev Cell.* 2003;5(1):45-57.
33. Guttmann-Raviv N, Shraga-Heled N, Varshavsky A, Guimaraes-Sternberg C, Kessler O, Neufeld G. Semaphorin-3A and semaphorin-3F work together to repel endothelial cells and to inhibit their survival by induction of apoptosis. *J Biol Chem.* 2007;282(36):26294-26305.
34. Chen J, Smith L. Retinopathy of prematurity. *Angiogenesis.* 2007;10(2):133-140.
35. Dorrell M, Friedlander M. Mechanisms of endothelial cell guidance and vascular patterning in the developing mouse retina. *Prog Retin Eye Res.* 2006;25(3):277-295.
36. Hou X, Roberts LJ II, Gobeil F Jr, et al. Isomer-specific contractile effects of a series of synthetic f2-isoprostanes on retinal and cerebral microvasculature. *Free Radic Biol Med.* 2004;36(2):163-172.
37. Chopp M, Zhang ZG, Jiang Q. Neurogenesis, angiogenesis, and MRI indices of functional recovery from stroke. *Stroke.* 2007;38(2 suppl):827-831.
38. Li L, Jiang Q, Zhang L, et al. Angiogenesis and improved cerebral blood flow in the ischemic boundary area detected by MRI after administration of sildenafil to rats with embolic stroke. *Brain Res.* 2007;1132(1):185-192.
39. Fulton AB, Hansen RM, Moskowitz A, Akula JD. The neurovascular retina in retinopathy of prematurity. *Prog Retin Eye Res.* 2009;28(6):452-482.
40. Frassetto LJ, Schlieve CR, Lieven CJ, et al. Kinase-dependent differentiation of a retinal ganglion cell precursor. *Invest Ophthalmol Vis Sci.* 2006;47(1):427-438.
41. Sun Q, Zhou H, Binmadi NO, Basile JR. Hypoxia-inducible factor-1-mediated regulation of semaphorin 4D affects tumor growth and vascularity. *J Biol Chem.* 2009;284(46):32066-32074.
42. Barisani D, Meneveri R, Ginelli E, Cassani C, Conte D. Iron overload and gene expression in HepG2 cells: analysis by differential display. *FEBS Lett.* 2000;469(2-3):208-212.
43. Martin G, Schlunck G, Hansen LL, Agostini HT.

Differential expression of angioregulatory factors in normal and CNV-derived human retinal pigment epithelium. *Graefes Arch Clin Exp Ophthalmol.* 2004;242(4):321-326.

44. Fujita H, Zhang B, Sato K, Tanaka J, Sakanaka M. Expressions of neuropilin-1, neuropilin-2 and semaphorin 3A mRNA in the rat brain after middle cerebral artery occlusion. *Brain Res.* 2001;914(1-2):1-14.
45. Carmichael ST. Cellular and molecular mechanisms of neural repair after stroke: making waves. *Ann Neurol.* 2006;59(5):735-742.
46. Carmichael ST, Archibeque I, Luke L, Nolan T, Momiy J, Li S. Growth-associated gene expression after stroke: evidence for a growth-promoting region in peri-infarct cortex. *Exp Neurol.* 2005; 193(2):291-311.
47. De Winter F, Oudega M, Lankhorst AJ, et al. Injury-induced class 3 semaphorin expression in the rat spinal cord. *Exp Neurol.* 2002;175(1):61-75.
48. Geretti E, Klagsbrun M. Neuropilins: novel targets for anti-angiogenesis therapies. *Cell Adh Migr.* 2007;1(2):56-61.
49. Casazza A, Finisguerra V, Capparuccia L, et al. Sema3E-Plexin D1 signaling drives human cancer cell invasiveness and metastatic spreading in mice. *J Clin Invest.* 120(8):2684-2698.
50. Robinson GS, Ju M, Shih SC, et al. Nonvascular role for VEGF: VEGFR-1, 2 activity is critical for neural retinal development. *FASEB J.* 2001;15(7): 1215-1217.
51. Alon T, Hemo I, Itin A, Pe'er J, Stone J, Keshet E. Vascular endothelial growth factor acts as a survival factor for newly formed retinal vessels and has implications for retinopathy of prematurity. *Nat Med.* 1995;1(10):1024-1028.
52. Schlingemann RO, Witmer AN. Treatment of retinal diseases with VEGF antagonists. *Prog Brain Res.* 2009;175:253-267.
53. Michaelson I. The mode of development of the vascular system of the retina with some observations on its significance for certain retinal disorders. *Trans Ophthalmol Soc UK.* 1948;68:137-180.
54. Campbell K. Intensive oxygen therapy as a possible cause of retrolental fibroplasia; a clinical approach. *Med J Aust.* 1951;2(2):48-50.
55. Lundbaek K, Christensen NJ, Jensen VA, et al. Diabetes, diabetic angiopathy, and growth hormone. *Lancet.* 1970;2(7664):131-133.
56. D'Amore PA, Sweet E. Effects of hyperoxia on microvascular cells in vitro. *In Vitro Cell Dev Biol.* 1987;23(2):123-128.
57. Smith LE. Pathogenesis of retinopathy of prematurity. *Growth Horm IGF Res.* 2004;14(suppl A): S140-S144.